JOURNAL OF APPLIED PHYSICS **121**, 044301 (2017)

On the domain size effect of thermal conductivities from equilibrium and nonequilibrium molecular dynamics simulations

Zuyuan Wang and Xiulin Ruan[a)]
School of Mechanical Engineering and the Birck Nanotechnology Center, Purdue University, West Lafayette, Indiana 47907, USA

(Received 1 October 2016; accepted 12 January 2017; published online 24 January 2017)

Equilibrium molecular dynamics (EMD) simulations with the Green-Kubo formula and nonequilibrium molecular dynamics (NEMD) simulations with the Fourier's Law are two widely used methods for calculating thermal conductivities of materials. It is well known that both methods suffer from domain size effects, especially for NEMD. But the underlying mechanisms and their comparison have not been much quantitatively studied before. In this paper, we investigate their domain size effects by using crystalline silicon at 1000 K, graphene at 300 K, and silicene at 300 K as model material systems. The thermal conductivity of silicon from EMD simulations increases normally with the increasing domain size and converges at a size of around $4 \times 4 \times 4\,\mathrm{nm}^3$. The converging trend agrees well with the wavelength-accumulated thermal conductivity. The thermal conductivities of graphene and silicene from EMD simulations decrease abnormally with the increasing domain size and converge at a size of around $10 \times 10\,\mathrm{nm}^2$. We ascribe the anomalous size effect to the fact that as the domain size increases, the effect of more phonon scattering processes (particularly the flexural phonons) dominates over the effect of more phonon modes contributing to the thermal conductivity. The thermal conductivities of the three material systems from NEMD simulations all show normal domain size effects, although their dependences on the domain size differ. The converging trends agree with the mean free path accumulation of thermal conductivity. This study provides new insights that other than some exceptions, the domain size effects of EMD and NEMD are generally associated with wavelength and mean free path accumulations of thermal conductivity, respectively. Since phonon wavelength spans over a much narrower range than mean free path, EMD usually has less significant domain size effect than NEMD. *Published by AIP Publishing.* [http://dx.doi.org/10.1063/1.4974884]

I. INTRODUCTION

Thermal conductivity is an important thermophysical property relevant to thermal management[1] and thermoelectrics[2] applications. Thermal conductivities of bulk materials can often be calculated with one of the following two methods: (1) equilibrium molecular dynamics (EMD) simulations with the Green-Kubo formula (hereafter referred to as the EMD method)[3–6] and (2) nonequilibrium molecular dynamics (NEMD) simulations with the Fourier's Law (hereafter referred to as the NEMD method).[3,7,8] In the EMD method, which is derived from statistical principles and the fluctuation-dissipation theorem,[6,9] the thermal conductivity is calculated as the integration of the heat current autocorrelation function (HCACF). In this method, the material systems under consideration always remain in equilibrium with no temperature gradient beyond thermal fluctuations, and the calculated thermal conductivity corresponds to a well-defined temperature. The NEMD method, on the other hand, is based on the Fourier's Law of heat conduction, which expresses thermal conductivity as the ratio of heat flux to temperature gradient.

It is well known that thermal conductivities calculated with both the EMD and NEMD methods suffer from domain size effects, especially for NEMD.[3] A general explanation for EMD is that as the domain size increases, more long-wavelength phonons become available to contribute to the thermal conductivity. The size effect with the EMD method usually disappears when the domain size increases to a few nanometers. The convergence at such small domain sizes has been attributed to the equilibrium nature of EMD simulations, which introduce no external disturbance to the phonons, and the periodic boundary conditions, which allow phonons to re-enter the domain.[10,11] The domain size effect with the NEMD method, on the other hand, could extend to a much larger domain size. For example, it has been shown that even for a domain size of around 10 μm, the thermal conductivity of graphene and silicon still changes with the domain size.[12,13] The NEMD domain size effect has been attributed to phonon scattering caused by the thermostats, which suppress the contribution of those long mean-free-path phonons.[3] However, a quantitative study of the relationship between the domain size effects of EMD/NEMD and the wavelength/mean free path accumulations of thermal conductivity, which could contribute to a more complete understanding of the underlying mechanism for the domain size effect on thermal conductivity, has not been done yet.

In this study, we considered silicon at 1000 K, graphene at 300 K, and silicene at 300 K as model material systems and investigated the domain size effect of their lattice

a)ruan@purdue.edu

thermal conductivities calculated with the EMD and NEMD methods. We also performed spectral energy density (SED) analysis on the materials to extract the spectral phonon properties, based on which we obtained the thermal conductivity accumulation profiles as a function of the phonon wavelength or mean free path. We examined the different domain size effects of the three materials and gained new insights. This paper is organized as follows. Section II details the methods used in this study, including the equilibrium and nonequilibrium molecular dynamics simulations, spectral energy density analysis, and thermal conductivity accumulation calculations. Section III presents the results on silicon, graphene, and silicene, as well as some discussion. Section IV summarizes the findings from this study.

II. METHODOLOGY

The molecular dynamics simulations were conducted with the LAMMPS package,[14] while the spectral analysis and thermal conductivity accumulation calculations were performed with some in-house code, which is also available on nanoHUB.[15] The interatomic interactions in graphene are characterized with an optimized Tersoff potential,[16] and those in silicene and silicon are characterized with the original Tersoff potential.[17,18] We noticed that Zhang *et al.* have optimized the Stillinger-Weber potential for silicene.[19] But the choice of potential is not to affect our comparisons between MD and phonon normal mode analysis, as long as the same potential is used in both calculations.

A. Equilibrium molecular dynamics simulations

Equilibrium molecular dynamics (EMD) simulations in combination with the Green-Kubo formula is an effective method for calculating lattice thermal conductivities of materials.[3–6] In this method, the thermal conductivity is calculated as[4]

$$k_{\alpha\beta} = \frac{V}{k_B T^2}\int_0^\infty \langle J_\alpha(0) J_\beta(t)\rangle \mathrm{d}t, \tag{1}$$

where $k_{\alpha\beta}$ is the $\alpha\beta$th component of the thermal conductivity tensor, V is the volume of the material system, k_B is the Boltzmann constant, T is temperature, t is time, and J_α is the αth component of the full heat current vector $\mathbf{J}$, which is computed as[14]

$$\mathbf{J} = \frac{1}{V}\left(\sum_i \mathbf{v}_i \epsilon_i + \sum_i \mathbf{S}_i \cdot \mathbf{v}_i\right), \tag{2}$$

where $\mathbf{v}_i$, ϵ_i, and $\mathbf{S}_i$ are the velocity, energy, and stress of atom i. In real practice, the integration upper limit "∞" in Eq. (1) is usually replaced by a finite number, $t_{\mathrm{corre,UL}}$, which we define as the upper limit of the correlation time. When $\alpha = \beta$, the term "$\langle J_\alpha(0) J_\beta(t)\rangle$" in Eq. (1) is called the heat current autocorrelation function (HCACF). Based on some reasoning on the thermodynamics of irreversible processes or the material structure related symmetries, it has been argued that the thermal conductivity tensor has to be symmetric.[20,21] For an isotropic material, the thermal conductivity tensor further reduces to a scalar, which, in MD simulations, is typically considered as $(k_x + k_y)/2$ (for two dimensional (2D) materials) or $(k_x + k_y + k_z)/3$ (for three dimensional (3D) materials). It should be noted that in this study, we used the default heat current formula implemented in LAMMPS, which is based on the per-atom stress.[14] Recently, Fan *et al.*[22] have reported that there are more accurate formulas for many-body potentials. However, the surprising domain size converging trend for graphene observed here is consistent with that under their new formula.

All the EMD simulations were conducted with a similar procedure. We applied periodic boundary conditions in the x, y, and z directions. The material systems were first equilibrated in an NPT (constant number of atoms, pressure, and temperature) ensemble by using Nosé-Hoover barostats and thermostats[23,24] for a duration of t_{NPT} to achieve a pressure of 0 bar and a desired temperature. After that, the material system was switched to an NVE (constant number of atoms, volume, and energy) ensemble to run for a duration of t_{NVE} for data production. The atomic trajectories were dumped every 10 steps. The upper limit of the heat current autocorrelation time was set to be $t_{\mathrm{corre,UL}}$, which was determined from some trial simulations and verified to provide converged thermal conductivities. In calculating the volume of material systems, we used a nominal thickness of 3.35 Å for graphene[25,26] and 4.2 Å for silicene.[18,19] For a fair comparison with the previous studies,[25,26] no quantum correction was performed to the thermal conductivities. To reduce statistical uncertainties, we ran each simulation five times, which had independent initial atomic velocity distributions. The reported thermal conductivities and error bars were calculated as the averages and standard deviations of the repetitive simulations, respectively. Note that the thermal conductivities were also averaged over the x, y, and z directions (for silicon) or x and y directions (for graphene and silicene). We noticed that graphene and silicene are anisotropic materials. In this study, our focus was on evaluating the average in-plane thermal conductivities, which are typically of greater importance to engineering applications than the chirality-dependent thermal conductivities. This treatment has been adopted in previous studies.[22,25] Many experimental measurements also assumed isotropic in-plane thermal conductivity such as the Raman measurements.[27] This is partly due to the fact that the anisotropy of the thermal conductivities of graphene and silicene along the zigzag and armchair directions is relatively small (<35%).[18,28] For general anisotropic materials (e.g., graphite and bismuth telluride), the domain size effect study should be conducted for each of the characteristic directions individually. Some critical simulation parameters are summarized in Table I.

B. Nonequilibrium molecular dynamics simulations

Nonequilibrium molecular dynamics (NEMD) simulations in combination with the Fourier's Law is another effective method for calculating lattice thermal conductivities of materials.[3,18] In this method, the thermal conductivity in a particular direction x is calculated as

TABLE I. Summary of critical parameters related to the EMD and NEMD simulations.

Material	Silicon	Graphene		Silicene	
Simulation type	EMD	EMD	NEMD	EMD	NEMD
Initial material structure	$L_c = 5.43$ Å	$L_{C-C} = 1.42$ Å		$L_{Si-Si} = 2.3$ Å (Ref. 29)	
	FCC lattice	Hexagonal lattice		Hexagonal lattice	
	3D	2D		Buckling: 0.44 Å (Ref. 29)	
Layer thickness (Å)	N.A.	3.35 (Refs. 25 and 26)		4.2 (Refs. 18 and 19]	
Min domain size (nm^3)	$1.1 \times 1.1 \times 1.1$	$2.1 \times 2.2 \times 2$	$4.3 \times 16.2 \times 20$	$1.3 \times 1.1 \times 2$	$6.6 \times 5.7 \times 20$
Max domain size (nm^3)	$10.3 \times 10.3 \times 10.3$	$16.2 \times 16.2 \times 2$	$512.0 \times 16.2 \times 20$	$30.4 \times 30.1 \times 2$	$149.6 \times 5.7 \times 20$
Atomic mass (a.u.)	28.0855	12.0107		28.0855	
Temperature (K)	1000	300		300	
Interatomic potential	Tersoff[17]	Optimized Tersoff[16]		Tersoff[17]	
Time step (fs)	1.0	0.5		0.6	
t_{NPT} (ns)	1.0	0.3	0.5	0.3	0.6
t_{NVE} (ns)	5.0	5.0	5.0	6.0	6.0
$t_{\text{corre,UL}}$ (ps)	150	100	N.A.	30	N.A.
k (W/m K)	$(k_x + k_y + k_z)/3$	$(k_x + k_y)/2$		$(k_x + k_y)/2$	
# of repetitions	5	5	5	5	5

$$k_x = \frac{q''}{|dT/dx|}, \tag{3}$$

where q'' is the heat flux and $|dT/dx|$ is the magnitude of the temperature gradient, both in the x direction.

All the NEMD simulations were conducted with a similar procedure. We applied fixed boundary conditions in the transport direction (x) and periodic boundary conditions in the two other directions (y and z). The material systems were first equilibrated in an NPT ensemble by using Nosé-Hoover barostats and thermostats[23,24] for a duration of t_{NPT} to achieve a pressure of 0 bar and a desired temperature. After that, the material system was switched to an NVE ensemble to run for a duration of t_{NVE} for data production. The temperatures at the two ends of the simulation domain were controlled with Langevin thermostats to be $(T + 30\,\text{K})$ and $(T - 30\,\text{K})$, respectively. The atomic trajectories were dumped every 10 steps, and those from the last 2 ns were used to calculate the temperature gradients. Some critical simulation parameters are summarized in Table I. Note that no NEMD simulation was conducted for silicon because of the associated high computational cost and the many available data in the literature.

C. Spectral energy density analysis

Spectral energy density (SED) analysis[30–32] was performed to extract the spectral phonon relaxation times. In the SED analysis, the atomic trajectories from the EMD simulations were Fourier-transformed from the time domain to frequency domain. The details of the SED analysis could be found in the literature.[18,32–34] Similar to previous studies,[12,18] we made an isotropic assumption and focused on a high symmetry direction ($\Gamma - X$ for silicon and $\Gamma - M$ for graphene and silicene) by discretizing it with N_k $\mathbf{k}$ points. The relaxation time, τ, of a particular phonon mode $(\mathbf{k}, \nu)$ is calculated as $\tau(\mathbf{k}, \nu) = 1/[2\gamma(\mathbf{k}, \nu)]$, where $\gamma(\mathbf{k}, \nu)$ is the half-width at the half-maximum of an SED peak.

With the spectral phonon properties from the SED analysis, we calculated the lattice thermal conductivity in a direction x with a formula based on the Boltzmann transport equation under the relaxation time approximation, as[32]

$$k_x = \sum_{\mathbf{k}} \sum_{\nu} c_{\text{ph,eq}}(\mathbf{k}, \nu) v_{\text{g},x}^2(\mathbf{k}, \nu) \tau(\mathbf{k}, \nu), \tag{4}$$

where ν is an index for phonon polarizations, $c_{\text{ph,eq}}(\mathbf{k}, \nu) = N_{k,\text{eq}} k_B / V$ is the equivalent specific heat of the phonon mode $(\mathbf{k}, \nu)$ accounting for the isotropic assumption, $v_{\text{g},x}(\mathbf{k}, \nu)$ is the x-component of the phonon group velocity, which is calculated as the gradient of the phonon dispersion curves from GULP[35] with a central difference method,[18] and $\tau(\mathbf{k}, \nu)$ is the phonon relaxation time obtained from the SED analysis. The thermal conductivities calculated by using Eq. (4) were compared with those from the EMD simulations to provide a validation for the spectral phonon properties.

D. Thermal conductivity accumulation calculations

Besides the thermal conductivities and spectral phonon properties, we also calculated the thermal conductivity accumulation with the phonon wavelength or mean free path. From lattice dynamics, the wavelength, λ, of a phonon mode is related to the wavenumber (or the magnitude of the wavevector $\mathbf{k}$), k, as $\lambda = 2\pi/k$. Once the coordinates of the discrete $\mathbf{k}$ points are known, the phonon wavelengths could be readily calculated. The mean free path, Λ, of a phonon mode is related to the phonon group velocity and relaxation time as $\Lambda = v_g \tau$. Based on the spectral phonon wavelengths, group velocities, and relaxation times, the thermal conductivity accumulation with the phonon wavelength can be calculated as[36]

$$k_{\text{accum}}(\lambda^*) = \sum_{\mathbf{k}} \sum_{\nu} c_{\text{ph,eq}}(\mathbf{k}, \nu, \lambda) v_{\text{g,x}}^2(\mathbf{k}, \nu, \lambda) \times \tau(\mathbf{k}, \nu, \lambda) \quad \text{for } 0 \le \lambda \le \lambda^*, \tag{5}$$

where λ^* represents the upper bound of the phonon wavelength. Similarly, the thermal conductivity accumulation with the phonon mean free path can be calculated as[36]

$$k_{\text{accum}}(\Lambda^*) = \sum_{\mathbf{k}} \sum_{\nu} c_{\text{ph,eq}}(\mathbf{k},\nu,\Lambda) v_{\text{g,x}}^2(\mathbf{k},\nu,\Lambda) \times \tau(\mathbf{k},\nu,\Lambda) \quad \text{for } 0 \le \Lambda \le \Lambda^*, \tag{6}$$

where Λ^* represents the upper bound of the phonon mean free path.

III. RESULTS AND DISCUSSION

In this section, we present the results from this study, which are organized by the three materials—silicon, graphene, and silicene. For silicon and graphene, we show some typical HCACF profiles, the thermal conductivity values from the EMD and NEMD methods, the phonon dispersions, and the thermal conductivity accumulation profiles. For silicene, we only show the thermal conductivity values from the EMD and NEMD methods and thermal conductivity accumulation profiles, because the HCACF profiles and phonon dispersions of silicene are similar to those of graphene.

A. Silicon

Figure 1 shows the convergence history of the normalized HCACF for silicon of four different simulation domain sizes at 1000 K. It is seen that a $t_{\text{corre,UL}}$ of 150 ps is sufficient to ensure that the normalized HCACF profiles fluctuate around zero. As the domain size increases, the rate, at which the normalized HCACF converges, increases, and the area under the normalized HCACF curve increases slightly because the negative portion reduces. Since the area under the HCACF curve is directly related to the thermal conductivity, the convergence seen in Fig. 1 implies that the thermal conductivity increases with the increasing domain size and then converges. The inset of Fig. 1 shows a material system with a domain size of $2.2 \times 2.2 \times 2.2\,\text{nm}^3$, as an illustration of the cubic simulation domains considered for silicon in this study.

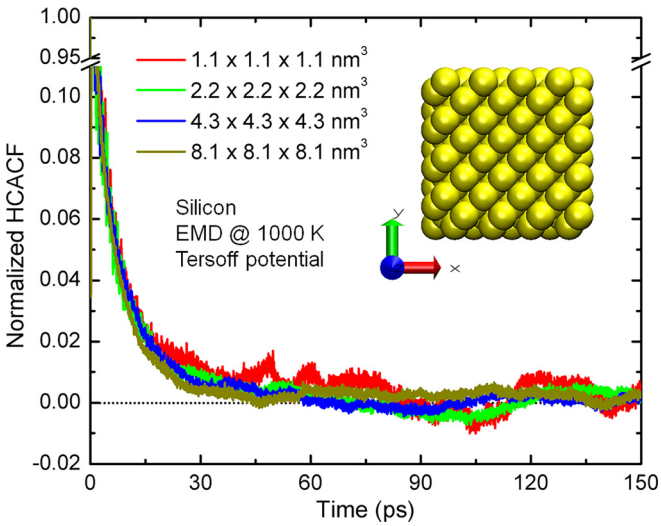

FIG. 1. Typical heat current autocorrelation function (HCACF) profiles of silicon at 1000 K for material systems of different sizes, normalized by the initial HCACF values. Each of the shown HCACF profiles is an average of five repetitive profiles. The inset shows a material system with a domain size of $2.2 \times 2.2 \times 2.2\,\text{nm}^3$.

In Fig. 2, we show the thermal conductivity from EMD and NEMD simulations of silicon at 1000 K. The thermal conductivity of silicon from EMD simulations increases with the domain size, as expected. Phonons with wavelength longer than the domain size cannot be supported; hence increasing the domain size will allow more long-wavelength phonons to contribute to thermal conductivity. Meanwhile, due to the periodic boundary conditions used, only a finite number of phonon modes are supported in the simulation domain; hence increasing the domain size will allow for a larger number of phonons, which lead to more scattering processes. The domain size effect observed here clearly indicates that the effect of more phonon modes contributing to the thermal conductivity dominates over the effect of more phonon scattering processes. The thermal conductivity from the EMD simulations reaches a converged value at a domain length of around 4 nm. The thermal conductivity of silicon from NEMD simulations also increases with increasing domain size and converges at a much larger domain size than EMD. It was attributed to the fact that the thermostats used in NEMD scatter phonons and suppress the contribution of long mean free path phonons.[3] To quantitatively understand the domain size effect of EMD and NEMD, we have found that the domain-size-dependent thermal conductivities from the EMD and NEMD simulations agree reasonably well with the thermal conductivity accumulation profiles as a function of the phonon wavelength and mean free path, respectively. This demonstrates that the EMD domain size effect is associated with the phonon wavelength

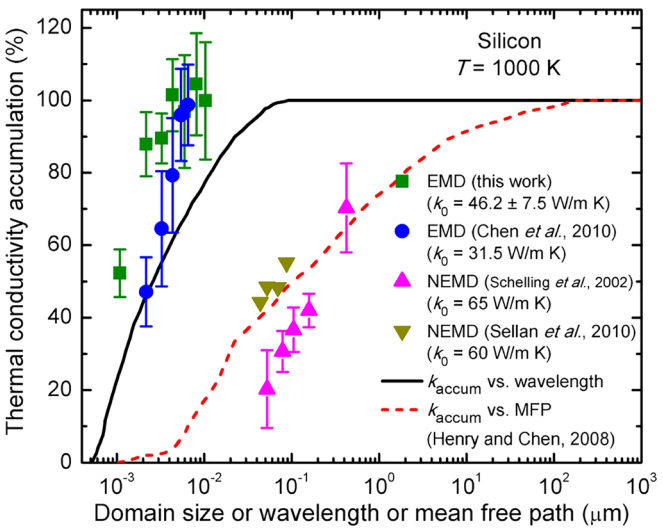

FIG. 2. Variation of the thermal conductivity of silicon at 1000 K with the simulation domain size or wavelength or mean free path. The square (green) and disk (blue) data points represent the thermal conductivities from our EMD simulations and those by Chen *et al.*,[37] respectively. The down-pointing (dark yellow) and up-pointing (magenta) triangle data points are the NEMD simulation results by Schelling *et al.*[3] and Sellan *et al.*,[38] respectively. The solid (black) and dashed (red) lines show the k_{accum} as a function of the phonon wavelength and mean free path by Henry and Chen,[12] respectively. The k_0 values indicate the converged thermal conductivities, which are used to normalize the thermal conductivities.

accumulation, while the NEMD domain size effect is associated with the mean free path accumulation. In EMD, the domain size limits the maximum wavelength that contributes to thermal conductivity, while the mean free path is not reduced due to the periodic boundary conditions.[11] In fact, the phonon scattering rates in EMD are underestimated due to the lack of scattering to the un-supported long wavelength phonons. On the other hand, in the wavelength accumulation plot, the scattering processes to the longer-wavelength phonons are always included. The fact that the EMD size effect agrees well with the wavelength accumulation indicates that the effect of the increased phonon modes contributing to the thermal conductivity dominates over the effect of the increased phonon scattering to the newly supported phonons. In NEMD, the domain size is typically large enough to support important phonon wavelengths, while the thermostats introduce phonon scattering and limit the phonon mean free path. Regarding the thermal conductivity of silicon at 1000 K, previous experiments gave 31.0 W/m K,[39] whereas the simulation results fall in the range 31.5–65 W/m K.[3,37,38] The discrepancies could be caused by the quality of the samples used in the experiments or the different empirical interatomic potentials used in the simulations. It is worth mentioning that the HCACF of silicon has a relatively slow decay, which requires a long correlation time to achieve an accurate prediction of the thermal conductivity. As temperature increases, the correlation time reduces. This is one of the reasons why the silicon simulations were conducted at 1000 K instead of 300 K. Another reason for the choice of the temperature is that there are more data for silicon at 1000 K available in the literature.

B. Graphene

Figure 3 shows the convergence history of the normalized HCACF for graphene of four different simulation domain sizes at 300 K. It is seen that at a $t_{corre,UL}$ of 100 ps the normalized HCACF decreases to about 1%, indicating that the choice of the $t_{corre,UL}$ is appropriate. As the domain size increases, the rate, at which the normalized HCACF converges, increases, and the area under the normalized HCACF curve decreases, gradually approaching a converged value. Since the area under the HCACF curve is directly related to the thermal conductivity, the convergence seen in Fig. 3 implies that the thermal conductivity decreases with the increasing domain size and then converges. The inset of Fig. 3 shows a material system with a domain size of $2.1 \times 2.2\,nm^2$, as an illustration of the nearly square simulation domains considered for graphene (and also silicene) in this study.

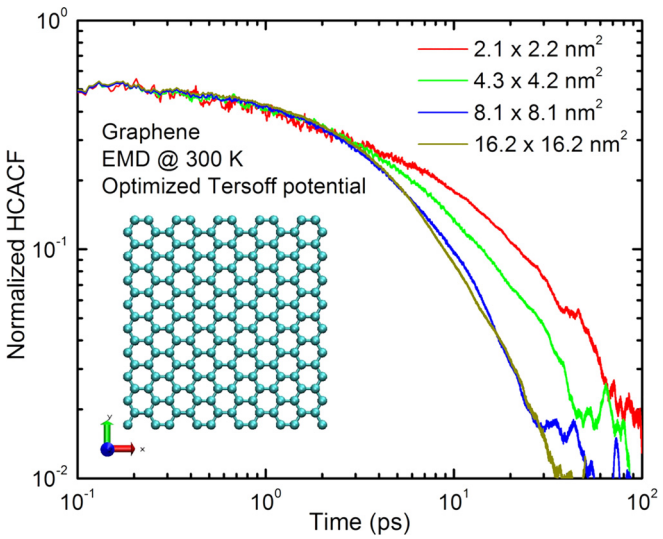

FIG. 3. Typical heat current autocorrelation function (HCACF) profiles of graphene at 300 K for material systems of different sizes, normalized by the initial HCACF values. Each of the shown HCACF profiles is an average of five repetitive profiles. The inset shows a material system with a domain size of $2.1 \times 2.2\,nm^2$.

Figure 4 shows our thermal conductivities of graphene at 300 K obtained from the EMD and NEMD simulations as a function of the simulation domain size. The EMD simulation results by Evans *et al.*[25] and those by Pereira and Donadio[26] are also shown as a comparison. The converged thermal conductivity from our EMD simulations is 1148 ± 129 W/m K, which agrees well with the value (1015 ± 120 W/m K) by Pereira and Donadio.[26] The much larger converged thermal conductivity (9164 ± 422 W/m K) by Evans *et al.*[25] could be attributed to the use of the original Tersoff potential.[17] It is clear that although the absolute thermal conductivity could depend on the potential, the variation of the normalized thermal conductivity with the domain size from our EMD simulations agrees well with those by Evans *et al.*[25] and by Pereira and Donadio,[26] all decreasing abnormally with the increasing domain size and reaching a converged value at a domain size of around 10 nm. This trend is also pointed out in a recent work by Fan *et al.*[22] We also observe that the converging

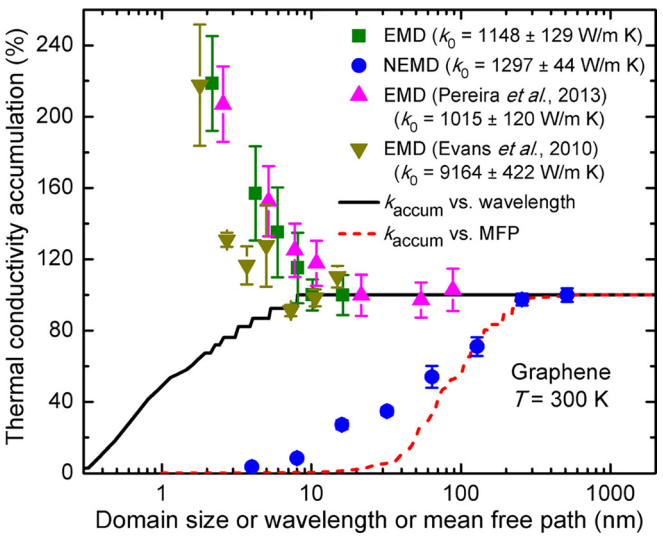

FIG. 4. Variation of the thermal conductivity of graphene at 300 K with the simulation domain size or wavelength or mean free path. The square (green) and disk (blue) data points represent the thermal conductivities from our EMD and NEMD simulations, respectively. The down-pointing (dark yellow) and up-pointing triangle (magenta) data points are the EMD simulation results by Evans *et al.*[25] and Pereira and Donadio,[26] respectively. The solid (black) and dashed (red) lines show the k_{accum} as a function of the phonon wavelength and mean free path, respectively. The k_0 values indicate the converged thermal conductivities, which are used to normalize the thermal conductivities.

trend is opposite to the wavelength accumulation of thermal conductivity. This anomalous size effect has been attributed to the dominating effect of more phonon scattering processes, particularly those associated with the low-frequency flexural phonons, over the effect of more phonon modes contributing to the thermal conductivity, as the domain size increases.[26] This is in contrast to the silicon results presented in Sec. III A, where the effect of the increased phonon modes contributing to the thermal conductivity dominates over the effect of the increased phonon scattering to the newly supported phonons.

To quantitatively show this point, we consider the spectral phonon relaxation times obtained from the SED analysis, as shown in Fig. 5 for two domain sizes, $4.3 \times 4.2\,\text{nm}^2$ and $16.2 \times 16.2\,\text{nm}^2$, respectively. When the size increases from $4.3 \times 4.2\,\text{nm}^2$ to $16.2 \times 16.2\,\text{nm}^2$, it can be seen that in general, the relaxation times of the ZA, TA, and LA phonons decrease, whereas those of the ZO, TO, and LO phonons remain relatively unchanged. Also, the phonon relaxation times generally decrease with the increasing phonon frequency. This is consistent with the analytical theory, which indicates that the phonon-phonon scattering rate (or the reciprocal of the phonon relaxation time) is related to the phonon frequency as ω^n, where n is a positive constant.[34] The relaxation times of the ZA, TA, and LA phonons are among the largest, suggesting their major roles in thermal transport. Because of limited scatterings, the relaxation times of the ZO phonons are also quite large, similar to the results in previous studies.[18,33] As a validation of the phonon relaxation time results, we point out that the total thermal conductivities from the SED analysis are 1674.3 and 1293.5 W/m K for the domain sizes of $4.3 \times 4.2\,\text{nm}^2$ and $16.2 \times 16.2\,\text{nm}^2$, respectively, which agree reasonably well with those from the EMD simulations. The slight discrepancies could be attributed to the relatively coarse sampling of the **k** points in the first Brillouin zone.

The thermal conductivity from the NEMD simulations increases with the increasing domain size, as expected, and converges at a domain size of around 500 nm. The converged thermal conductivity (1297 ± 44 W/m K) is in agreement with the converged thermal conductivity from our EMD simulations. This result is also consistent with a previous study, which states that for bulk (macroscopic) graphene, both EMD and NEMD simulations should provide a finite, similar thermal conductivity value.[22] The thermal conductivity accumulation with the phonon wavelength agrees well the EMD data, except for the opposite trends, whereas the thermal conductivity accumulation with the phonon mean free path agrees well with the NEMD data, similar to those of silicon.

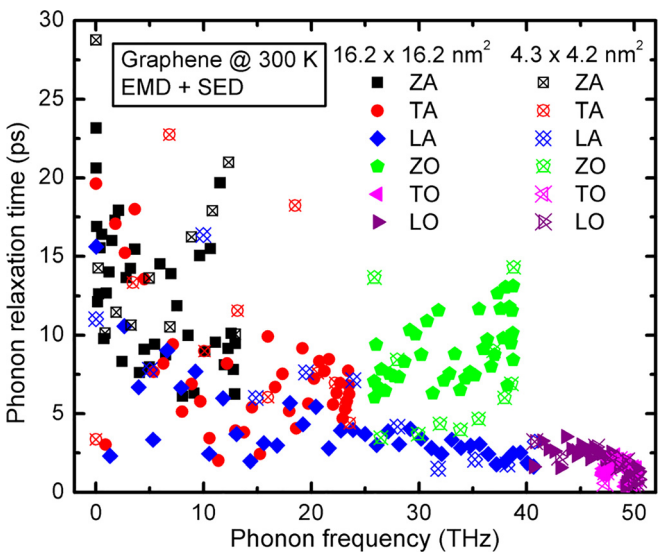

FIG. 5. Spectral phonon relaxation times in graphene at 300 K for two domain sizes, $4.3 \times 4.2\,\text{nm}^2$ and $16.2 \times 16.2\,\text{nm}^2$.

C. Silicene

We move on to discuss the results for silicene. The HCACF profiles of silicene are not shown because they are similar to those of graphene (see Fig. 3). In Fig. 6, we show the thermal conductivity results for silicene. It is seen that the thermal conductivity from the EMD simulations decreases abnormally with the increasing domain length and reaches a converged value at a domain length of around 10 nm, whereas that from the NEMD simulations increases normally with the increasing domain length. The thermal conductivity accumulation with the phonon wavelength agrees well the EMD data, except for the opposite trends, and the thermal conductivity accumulation with the phonon mean free path agrees well with the NEMD data. Considering that silicene has a similar structure to graphene, these results are expected. But we also observe a few discrepancies: (1) the thermal conductivity of silicene at 300 K is much lower than that of graphene at the same temperature, which could be attributed to the larger atomic mass of a silicon atom than a carbon atom and the weaker bonds in silicene than in graphene; (2) the variation (~50%) of the thermal conductivity of silicene from the EMD simulations

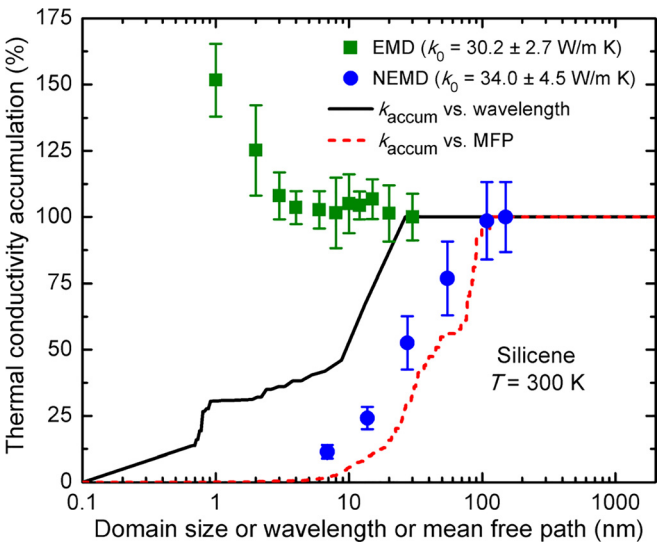

FIG. 6. Variation of the thermal conductivity of silicene at 300 K with the simulation domain size or wavelength or mean free path. The square (green) and disk (blue) data points represent the thermal conductivities from our EMD and NEMD simulations, respectively. The solid (black) and dashed (red) lines show the k_{accum} as a function of the phonon wavelength and mean free path, respectively. The k_0 values indicate the converged thermal conductivities, which are used to normalize the thermal conductivities.

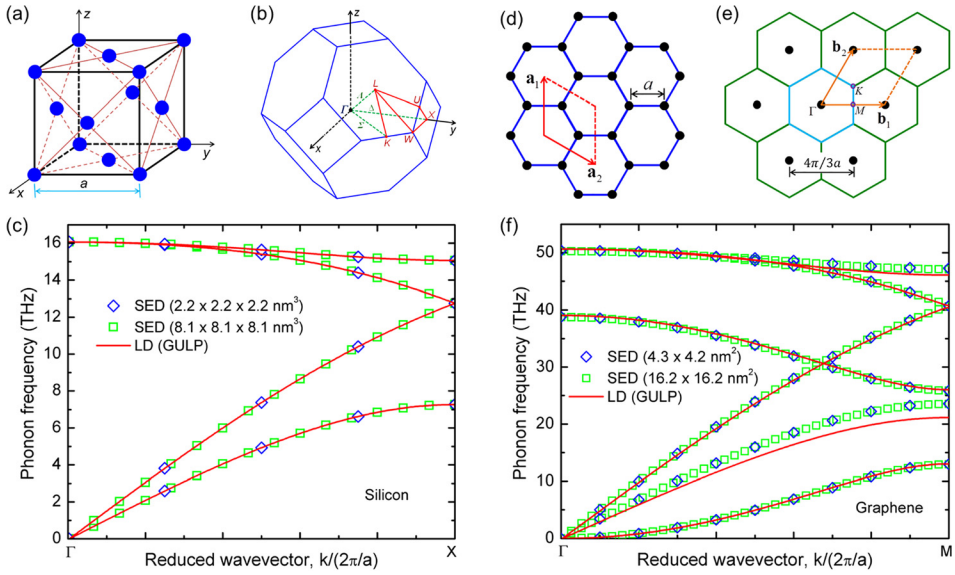

FIG. 7. (a) Schematic of the direct lattice of silicon. (b) Schematic of the reciprocal lattice of silicon. (c) Phonon dispersions of silicon along the $\Gamma - X$ direction. (d) Schematic of the direct lattice of graphene. (e) Schematic of the reciprocal lattice of graphene. The middle (cyan) hexagon shows the first Brillouin zone of graphene. (f) Phonon dispersions of graphene along the $\Gamma - M$ direction. For the phonon dispersions, the solid (red) lines are from the lattice dynamics calculations with GULP;[35] the diamond (blue) and square (green) data points are from the SED analysis of two material systems with different domain sizes.

is much smaller than the variation (~120%) of the thermal conductivity of graphene from the EMD simulations, which could be resulted from the smaller relative contributions of the flexural phonon modes to the thermal conductivity of silicene than graphene; (3) the thermal conductivity accumulation with the phonon mean free path for silicene converges within a much narrower range of mean free paths, which could be due to the smaller phonon mean free paths in silicene. In addition, it is worth pointing out that because of the buckling structure the polarization vectors of the flexural phonons in silicene are typically not perpendicular to the silicene 2D plane,[40] which could be another reason why the thermal conductivity of silicene from the EMD simulations suffers less from the domain size effect. Regarding the thermal conductivity of silicene, there seems to be no consensus so far, and the reported values vary from 8 to 43.4 W/m K.[18,19,41,42]

To examine the effect of the domain size on the number of available phonon modes, which is essential for evaluating the domain size effect, we calculated, by conducting SED analysis, the phonon dispersions corresponding to two different simulation domain sizes. In Fig. 7, we show (a) the direct lattice of silicon, (b) the reciprocal lattice of silicon, (c) the phonon dispersions of silicon along the $\Gamma - X$ direction, (d) the direct lattice of graphene, (e) the reciprocal lattice of graphene, and (f) the phonon dispersions of graphene along the $\Gamma - M$ direction. The phonon dispersions from the SED analysis are compared to those from the lattice dynamics calculations with GULP.[35] The good agreement indicates the weak dependence of the phonon dispersions on temperature, because the lattice dynamics calculations correspond to 0 K, while the SED analysis corresponds to 300 K. It is also seen that much more phonon modes are available in a larger domain than those in a smaller domain. The additional phonon modes associated with a larger domain have opposite effects in silicon and graphene. In silicon, the contributions of those phonon modes to the thermal conductivity exceed the increased phonon-phonon scattering processes, leading to a normal size effect of the thermal conductivity from EMD simulations; in graphene, the increased phonon-phonon scattering processes surpass the contributions to the thermal conductivity by those additional phonon modes, resulting in an abnormal size effect of the thermal conductivity from EMD simulations. Considering the different structures of silicon (3D) and graphene (2D), the different size effects are believed to result primarily from the low-frequency flexural phonon modes,[22] which have been shown to be the main contributors of thermal conductivity of graphene.[43] As the structure changes from graphene (2D) to silicene (quasi-2D), the abnormality of the domain size effect of the EMD results decreases.

Finally, we point out that our findings about the domain size effects of EMD and NEMD simulations apply mainly to crystalline materials that involve primarily phonon-phonon scattering processes. For amorphous materials or crystalline materials involving other significant phonon scattering processes (e.g., phonon-impurity, phonon-defect, phonon-interface, *etc.*), the domain size effects are expected to be more complicated. Additional work is needed to gain a deeper understanding of them.

IV. CONCLUSIONS

In summary, we have conducted EMD and NEMD simulations as well as phonon normal mode analysis to study the domain size effects of the thermal conductivities of silicon at 1000 K, graphene at 300 K, and silicene at 300 K. The thermal conductivity of silicon from the EMD simulations increases normally with the increasing domain size and converges at a size of around $4 \times 4 \times 4\,\text{nm}^3$. The normal size effect is resulted from the dominating effect of more phonon modes contributing to the thermal conductivity over the effect of more phonon scattering processes, as the domain size increases. Therefore, the converging trend agrees well with the wavelength accumulation of thermal conductivity. The thermal conductivities of graphene and silicene from the EMD simulations decrease abnormally with the increasing domain size and converge at a size of around $10 \times 10\,\text{nm}^2$. The anomalous size effect is due to the dominating effect of

more phonon scattering processes (particularly those associated with the low-frequency flexural phonons) over the effect of more phonon modes contributing to the thermal conductivity, as the domain size increases. Therefore, the converging trend has an opposite profile than the wavelength accumulation. The thermal conductivities of the three material systems from the NEMD simulations all show normal domain size effects, although their dependences on the domain size differ. The converging trend agrees well with the mean free path accumulation of thermal conductivity. This study provides new insights into the domain size effects of the thermal conductivities from EMD and NEMD simulations; it is potentially useful for similar studies on other material systems.

ACKNOWLEDGMENTS

We thank the support from the National Science Foundation (Award No. 1150948).

[1]S. Ghosh, I. Calizo, D. Teweldebrhan, E. P. Pokatilov, D. L. Nika, A. A. Balandin, W. Bao, F. Miao, and C. N. Lau, Appl. Phys. Lett. **92**, 151911 (2008).
[2]T. M. Tritt and M. A. Subramanian, MRS Bull. **31**, 188 (2006).
[3]P. K. Schelling, S. R. Phillpot, and P. Keblinski, Phys. Rev. B **65**, 144306 (2002).
[4]D. A. McQuarrie, *Statistical Mechanics* (University Science Books, Sausalito, 2000).
[5]M. S. Green, J. Chem. Phys. **22**, 398 (1954).
[6]R. Kubo, J. Phys. Soc. Jpn. **12**, 570 (1957).
[7]F. Muller-Plathe, J. Chem. Phys. **106**, 6082 (1997).
[8]P. Jund and R. Jullien, Phys. Rev. B **59**, 13707 (1999).
[9]R. Kubo, Rep. Prog. Phys. **29**, 255 (1966).
[10]J. Che, T. Cagin, W. Deng, and W. A. Goddard III, J. Chem. Phys. **113**, 6888 (2000).
[11]L. Sun and J. Y. Murthy, Appl. Phys. Lett. **89**, 171919 (2006).
[12]A. S. Henry and G. Chen, J. Comput. Theor. Nanosci. **5**, 141 (2008).
[13]X. Xu, L. F. C. Pereira, Y. Wang, J. Wu, K. Zhang, X. Zhao, S. Bae, C. T. Bui, R. Xie, J. T. L. Thong, B. H. Hong, K. P. Loh, D. Donadio, B. Li, and B. Ozyilmaz, Nat. Commun. **5**, 3689 (2014).
[14]S. Plimpton, J. Comput. Phys. **117**, 1 (1995).
[15]T. Feng and X. Ruan, see https://nanohub.org/resources/lorentzfit for a Lorentzian fitting tool for phonon spectral energy density (SED) calculations, accessed 18 September 2016.
[16]L. Lindsay and D. A. Broido, Phys. Rev. B **81**, 205441 (2010).
[17]J. Tersoff, Phys. Rev. B **37**, 6991 (1988).
[18]Z. Wang, T. Feng, and X. Ruan, J. Appl. Phys. **117**, 084317 (2015).
[19]X. Zhang, H. Xie, M. Hu, H. Bao, S. Yue, G. Qin, and G. Su, Phys. Rev. B **89**, 054310 (2014).
[20]H. B. G. Casimir, Rev. Mod. Phys. **17**, 343 (1945).
[21]C.-C. Wang, *On the Symmetry of the Heat-Conduction Tensor*, in *Rational Thermodynamics*, 2nd ed., edited by C. Truesdell (Springer-Verlag, New York, 1984).
[22]Z. Fan, L. F. C. Pereira, H. Q. Wang, J. C. Zheng, D. Donadio, and A. Harju, Phys. Rev. B **92**, 094301 (2015).
[23]S. Nosé, J. Chem. Phys. **81**, 511 (1984).
[24]W. G. Hoover, Phys. Rev. A **31**, 1695 (1985).
[25]W. J. Evans, L. Hu, and P. Keblinski, Appl. Phys. Lett. **96**, 203112 (2010).
[26]L. F. C. Pereira and D. Donadio, Phys. Rev. B **87**, 125424 (2013).
[27]A. A. Balandin, S. Ghosh, W. Bao, I. Calizo, D. Teweldebrhan, F. Miao, and C. N. Lau, Nano Lett. **8**, 902 (2008).
[28]Y. Wang, B. Qiu, and X. Ruan, Appl. Phys. Lett. **101**, 013101 (2012).
[29]S. Cahangirov, M. Topsakal, E. Aktrk, H. Sahin, and S. Ciraci, Phys. Rev. Lett. **102**, 236804 (2009).
[30]J. Shiomi and S. Maruyama, Phys. Rev. B **73**, 205420 (2006).
[31]N. de Koker, Phys. Rev. Lett. **103**, 125902 (2009).
[32]J. A. Thomas, J. E. Turney, R. M. Lutzi, C. H. Amon, and A. J. H. McGaughey, Phys. Rev. B **81**, 081411 (2010).
[33]B. Qiu and X. Ruan, Appl. Phys. Lett. **100**, 193101 (2012).
[34]T. Feng and X. Ruan, J. Nanomater. **2014**, 206370 (2014).
[35]J. D. Gale and A. L. Rohl, Mol. Simul. **29**, 291 (2003).
[36]Z. Wang and X. Ruan, Comput. Mater. Sci. **121**, 97 (2016).
[37]J. Chen, G. Zhang, and B. Li, Phys. Lett. A **374**, 2392 (2010).
[38]D. P. Sellan, E. S. Landry, J. E. Turney, A. J. H. McGaughey, and C. H. Amon, Phys. Rev. B **81**, 214305 (2010).
[39]C. J. Glassbrenner and G. A. Slack, Phys. Rev. **134**, A1058 (1964).
[40]H. Xie, M. Hu, and H. Bao, Appl. Phys. Lett. **104**, 131906 (2014).
[41]H. Li and R. Zhang, Europhys. Lett. **99**, 36001 (2012).
[42]M. Hu, X. Zhang, and D. Poulikakos, Phys. Rev. B **87**, 195417 (2013).
[43]L. Lindsay, D. A. Broido, and N. Mingo, Phys. Rev. B **82**, 115427 (2010).